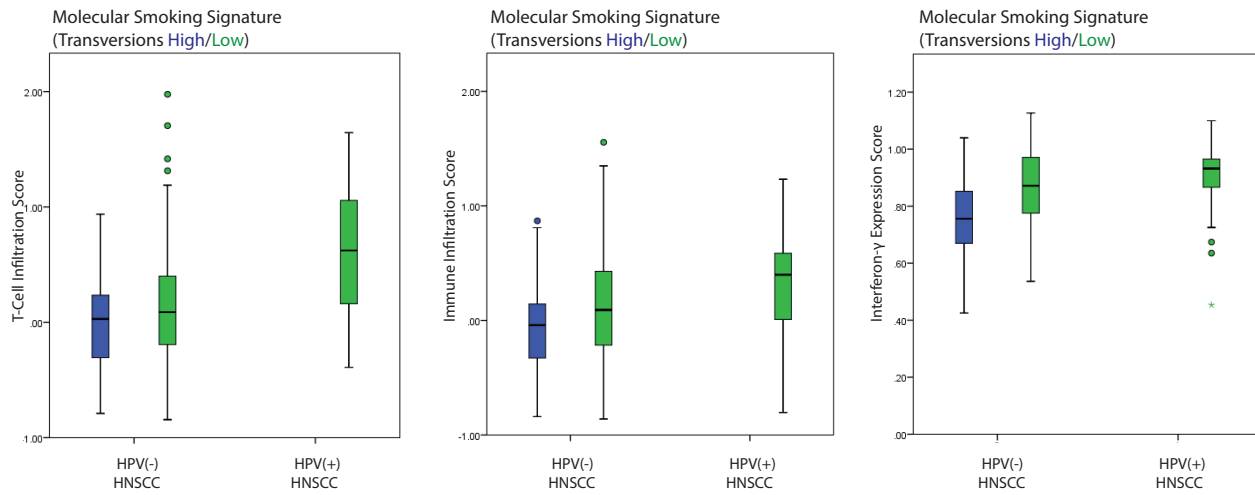
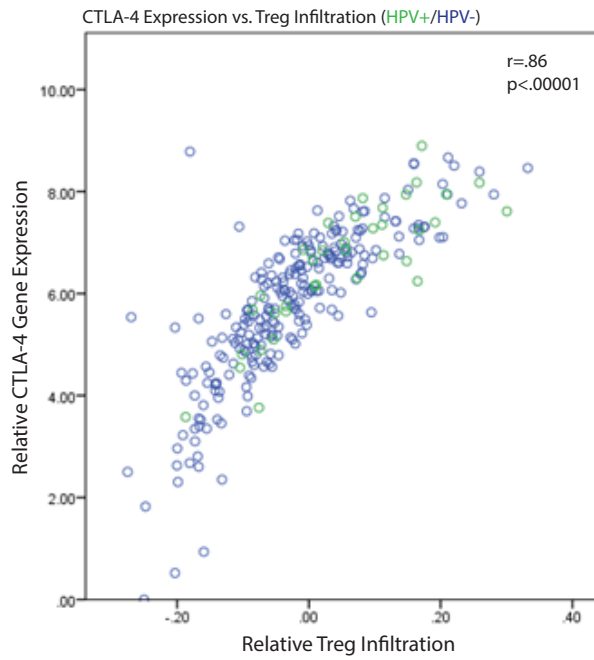


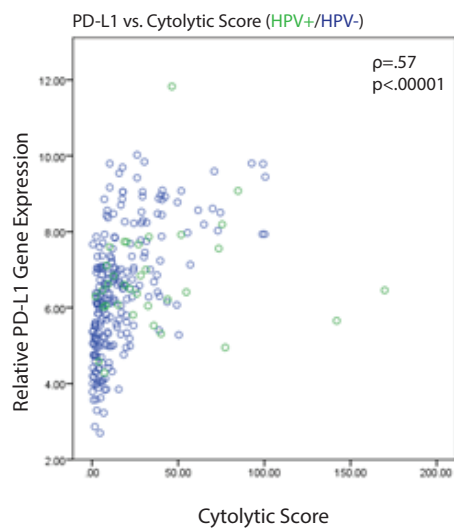
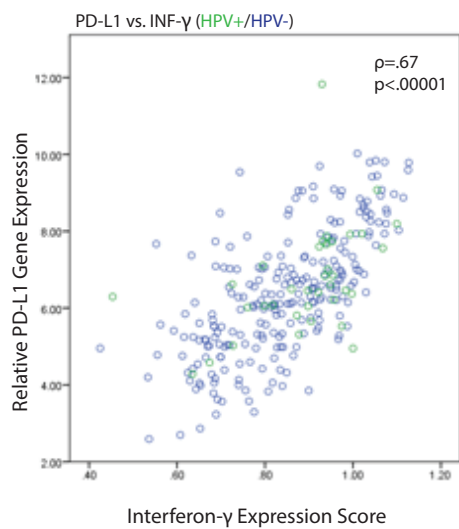
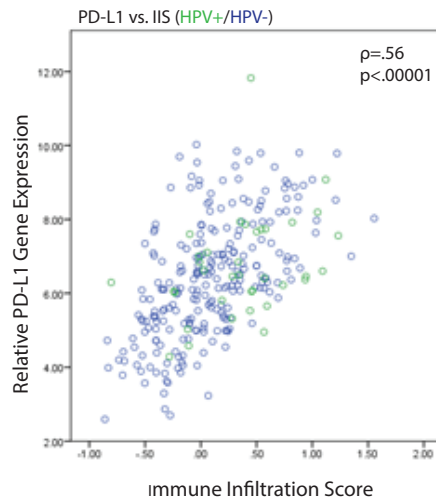
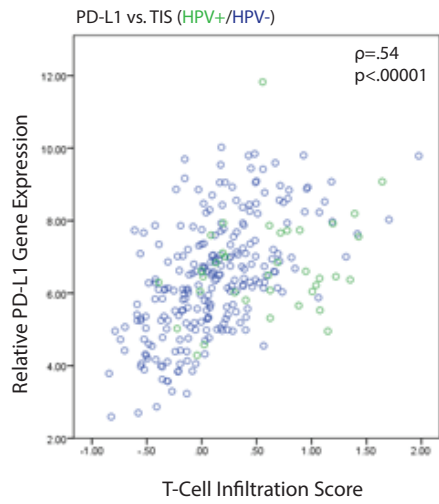
**Supplemental Figure 1.** Clinical Smoking History and Tumor Immune Infiltration. Patient clinical smoking history divided as current or recently reformed smokers (active smoker within last 15 years) vs. never or long-standing reformed smokers (active smoker greater than 15 years prior) correlated with T-cell infiltration (TIS), immune cell infiltration (IIS), and immune cytolytic score (CYT). All box-whisker plots represent values within the interquartile range (IQR) (boxes) and 1.5xIQR (whiskers). Outliers are plotted as values >1.5xIQR (circles) and >3xIQR (stars). All p-values for significance (<.05) represent comparisons via two-tailed t-tests.  $n=280$ .



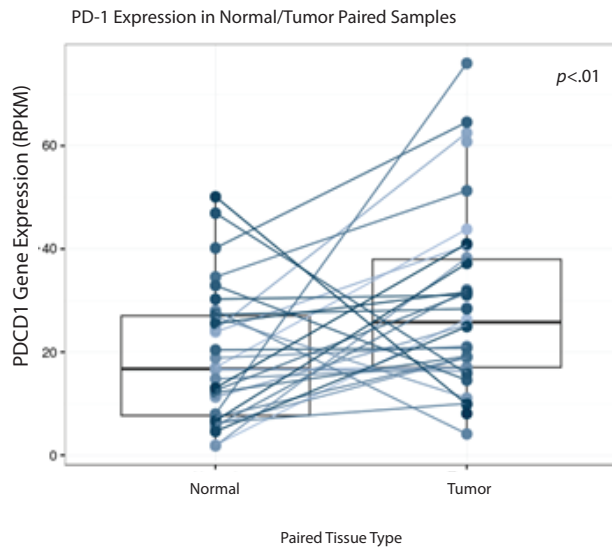
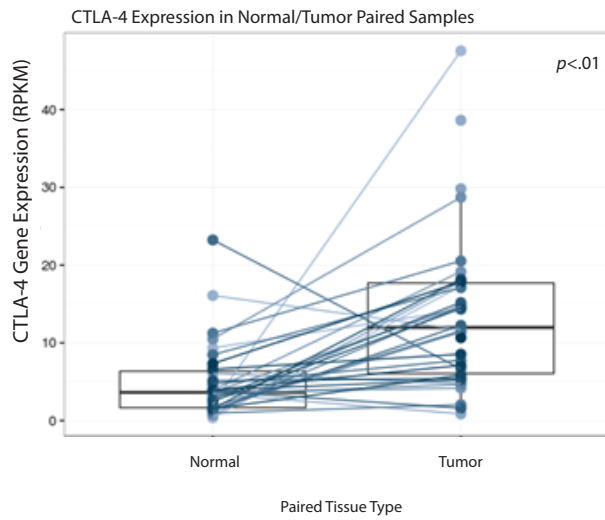
**Supplemental Figure 2. Nucleotide Transversion Molecular Smoking Signature and Immune Infiltration.** Clinical Smoking History and Tumor Immune Infiltration. T-cell infiltration (TIS), immune cell infiltration (IIS), and interferon- $\gamma$  expression scores correlated with nucleotide transversion high/low molecular smoking signatures in HPV positive and negative HNSCC tumors. All box-whisker plots represent values within the interquartile range (IQR) (boxes) and 1.5xIQR (whiskers). Outliers are plotted as values >1.5xIQR (circles) and >3xIQR (stars).  $n=280$ .



**Supplemental Figure 3. Correlations between PD-L1 Expression and Immune Infiltration and Activation Metrics.** Correlations between CTLA-4 gene expression and regulatory T-cell infiltration. All  $r$  values represent Pearson correlation coefficients. Two-tailed  $p$ -values are presented for significance ( $<.05$ ).  $n=280$ .

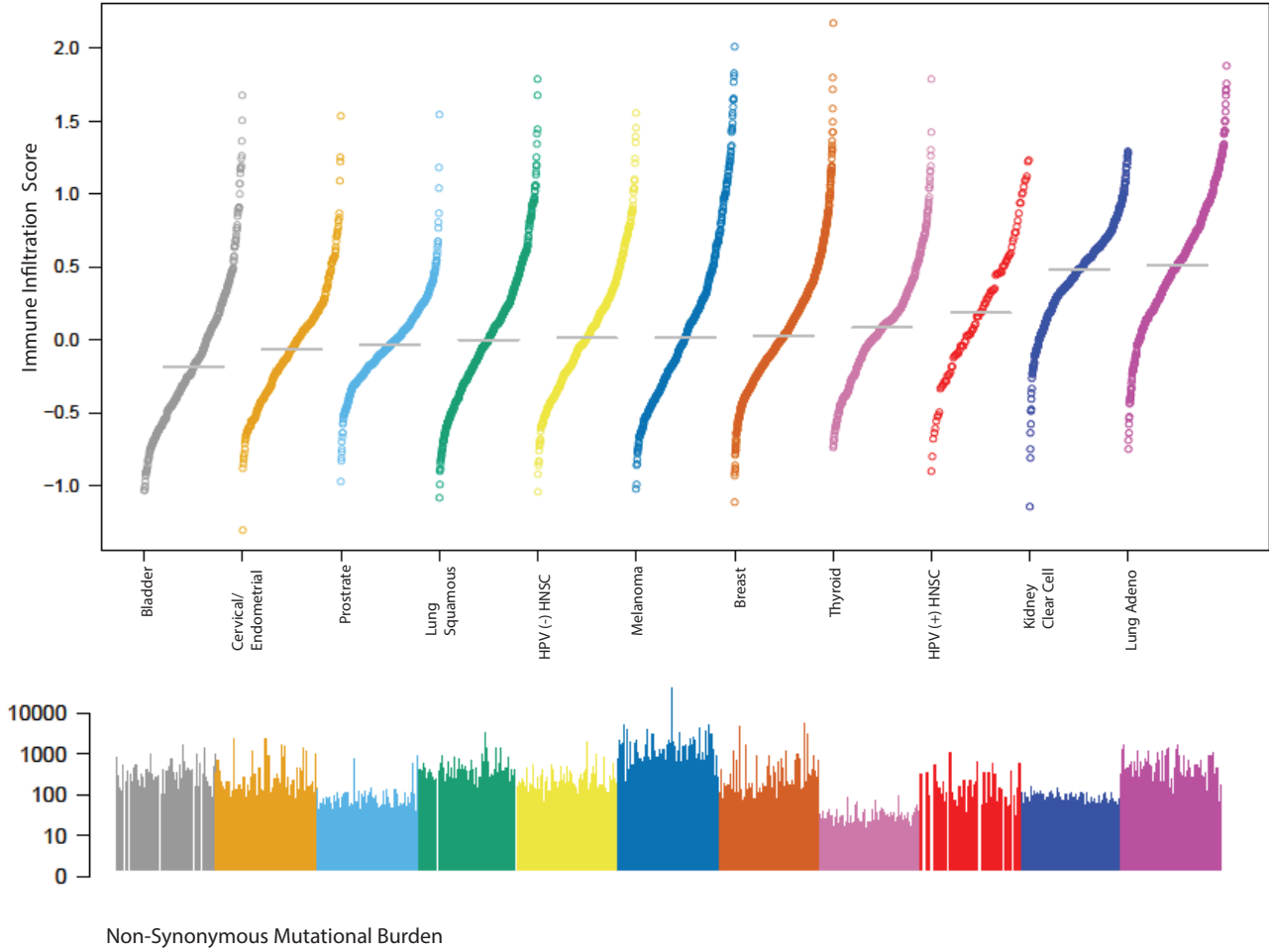


**Supplemental Figure 4. Correlations between PD-L1 Expression and Immune Infiltration and Activation Metrics.** Correlations between PD-L1 (CD274) expression and T-cell infiltration (TIS), overall immune cell infiltration (IIS), interferon- $\gamma$  expression score, and cytolytic score. All  $r$  values represent Spearman correlation coefficients. Two-tailed  $p$ -values are presented for significance ( $<.05$ ).  $n=280$ .

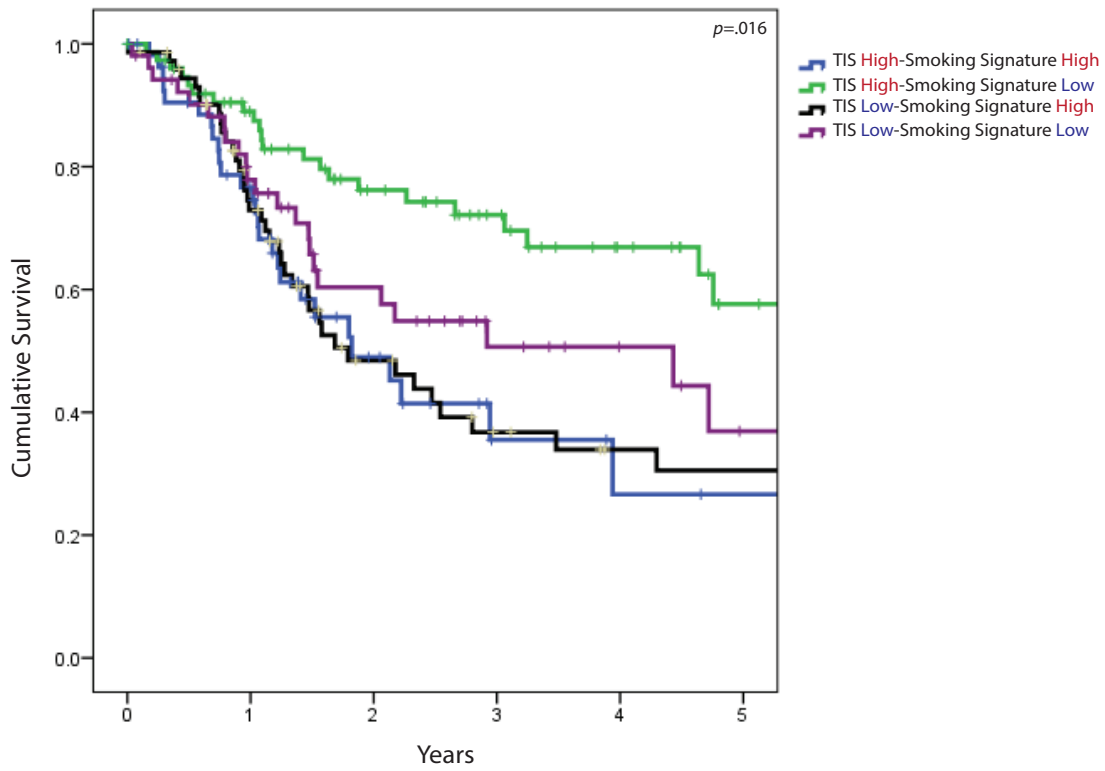


**Supplemental Figure 5. Comparison of CTLA-4 and PD-1 Expression in Normal and Tumor Matched Samples.** Gene expression of CTLA-4 and PDCD1 (PD-1) measured by RPKM (Reads Per Kilobase of transcript per Million mapped) of head and neck squamous tumors and patient matched normal tissue controls in 34 patients available from the TCGA HNSCC dataset.  $n=34$ . Paired Wilcoxon ranked test,  $p < .01$ .

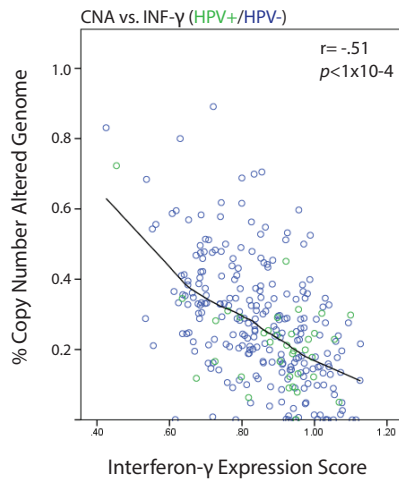
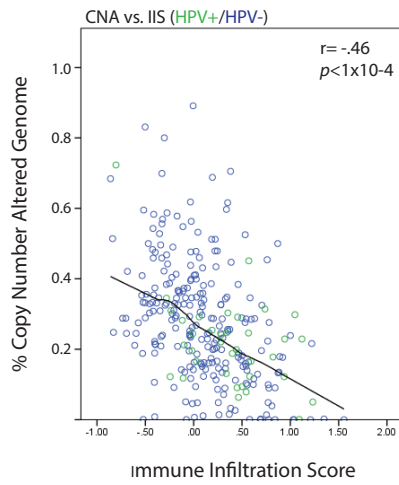
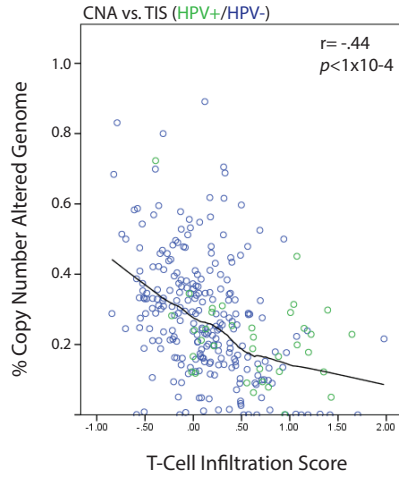
### Ten Most Immune Infiltrated Tumors



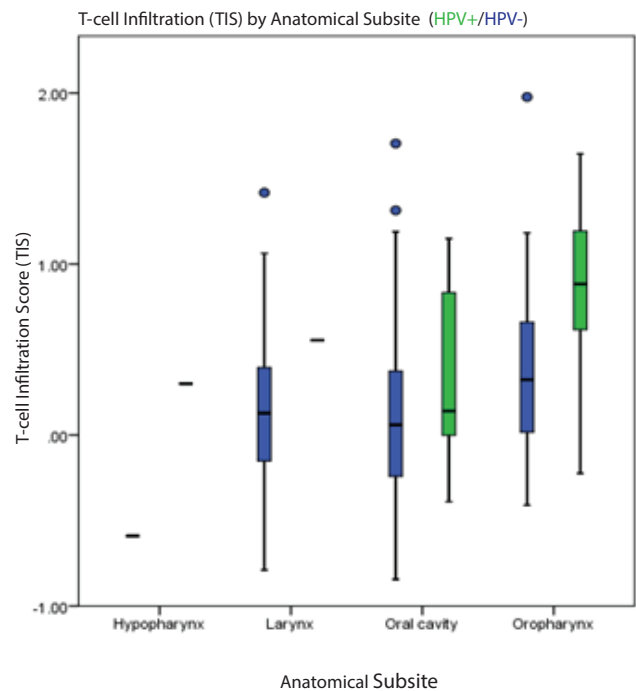
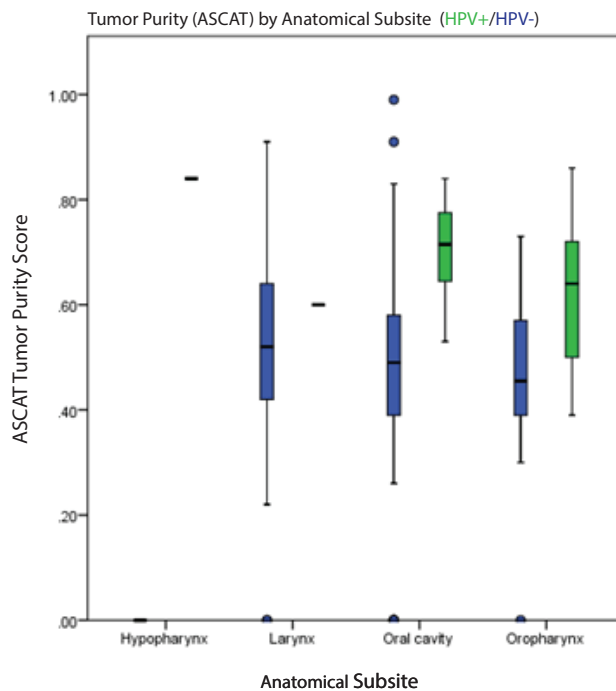
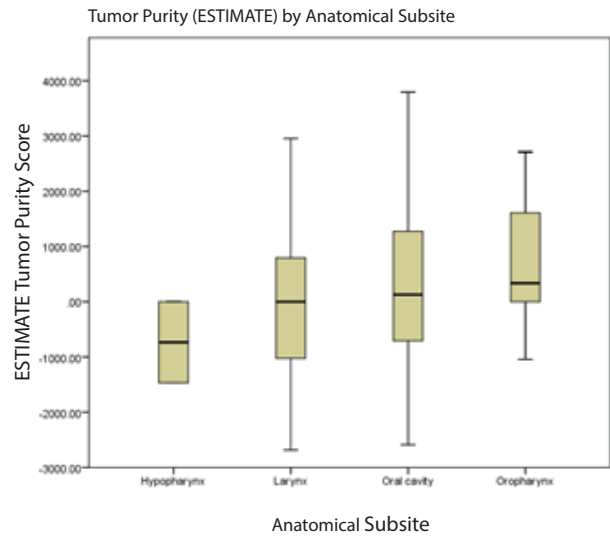
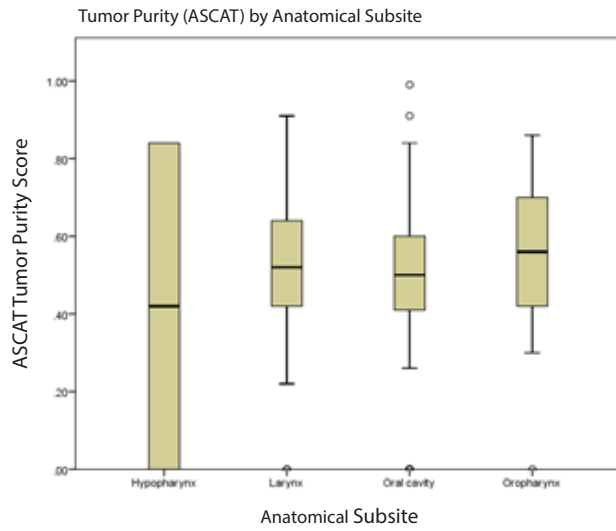
**Supplemental Figure 6. Immune Infiltration and Mutational Burden.** Relative median immune infiltration across the ten most immune infiltrated tumors in increasing order including HPV positive and negative HNSCC tumors with corresponding levels non-synonymous mutational burden below.



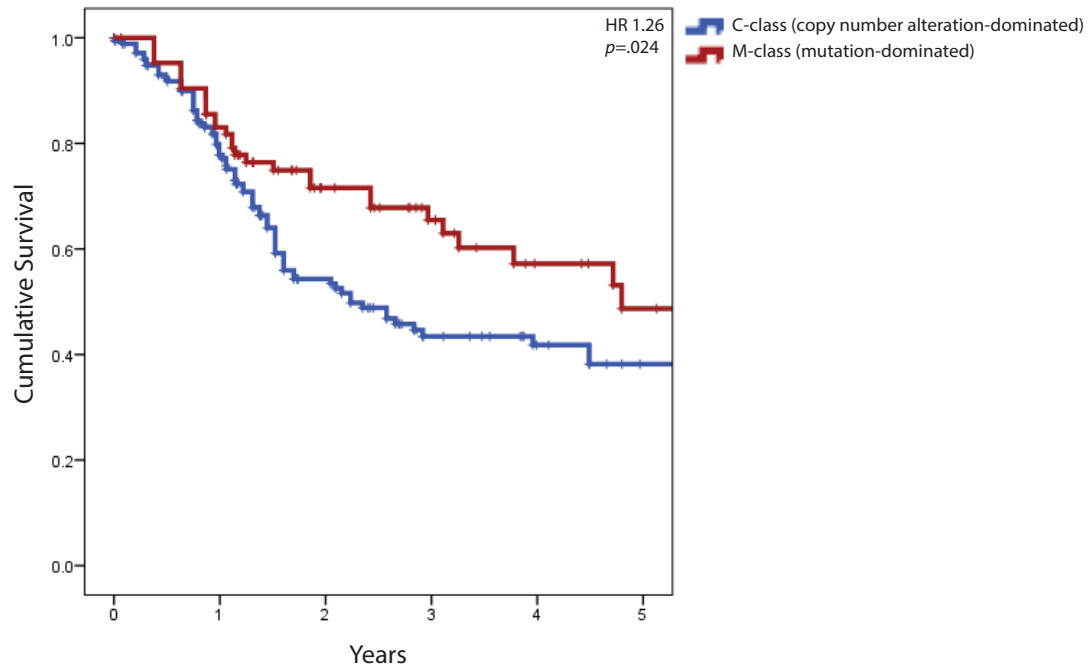
**Supplemental Figure 7. Impact of T-cell Infiltration and Smoking Status on HPV-Adjusted Overall Survival.** Correlations with patient cumulative survival and tumor T-cell infiltration (TIS) above/below median (high/low) and molecular smoking signature above/below median (high/low),  $n=280$ .



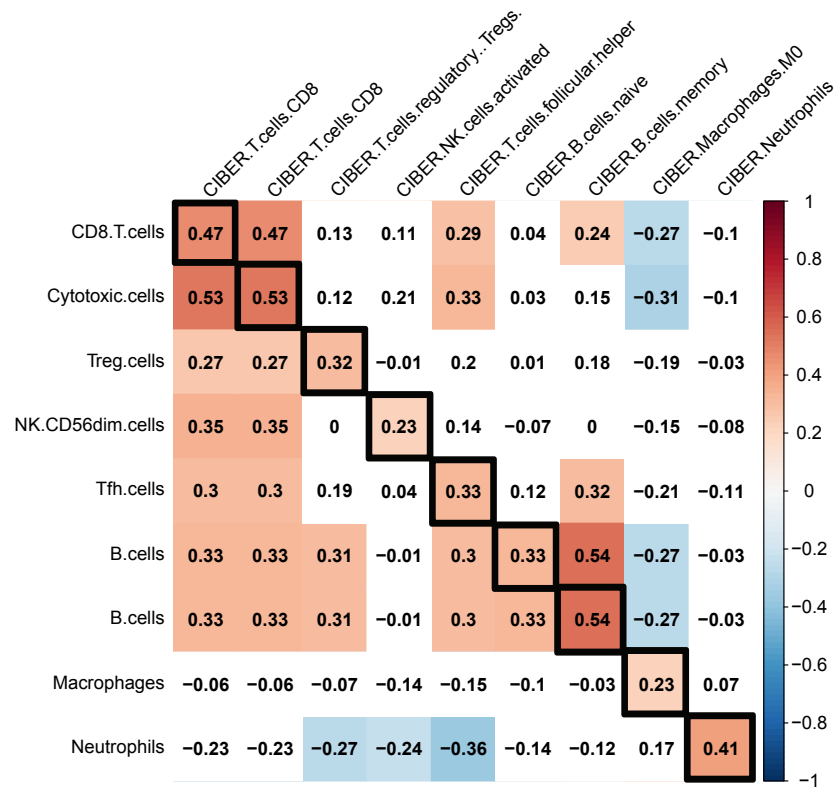
**Supplemental Figure 8. Percent Copy Number Altered Genome and Immune Infiltration Metrics.** Correlations between copy number alteration (the fraction of a tumor's genome copy number-altered with log2 copy number ratio  $<-.2$  or  $>.2$ ) and T-cell infiltration (TIS), overall immune cell infiltration (IIS), and interferon- $\gamma$  expression score. All r values represent Pearson correlation coefficients. Two-tailed p-values are presented for significance ( $<.05$ ).  $n=280$ .



**Supplemental Figure 9. Tumor Purity by Anatomical Subsite.** Relative tumor purity and t-cell infiltration (TIS) stratified by head and neck anatomical subsite. Relative tumor purity quantified with two independent computational tools (SNP6 copy-number based ASCAT and expression-based ESTIMATE) to infer tumor purity. All box-whisker plots represent values within the interquartile range (IQR) (boxes) and 1.5xIQR (whiskers). Outliers are plotted as values >1.5xIQR (circles) and >3xIQR (stars).  $n=280$ .



**Supplemental Figure 10. C-class (Copy Number Alteration-dominated) vs. M-class (Mutation-Dominated) Tumors and Patient Survival.** Correlations with patient cumulative survival and copy number alteration dominated tumors as compared to mutation dominated tumors. P values for significance ( $<.05$ ) calculated using multivariable Cox regression analysis.  $n=280$ .



Immune Cell Score Comparison Groups	Pearson r-coefficient	p-value (n=242)
CD8+ T-cell vs. CD8+ T-cell (CIBERSORT)	0.47	<0.00001
CD8+ CTL T-cell vs. CD8+ T-cell (CIBERSORT)	0.53	<0.00001
T-Regulatory Cell vs. T-Regulatory Cell (CIBERSORT)	0.32	<0.00001
CD56dim NK Cell vs. Activated NK Cell (CIBERSORT)	0.23	0.0003
Follicular T-Helper Cell vs. Follicular T-Helper Cell (CIBERSORT)	0.33	<0.00001
B Cell vs. Naïve B Cell (CIBERSORT)	0.33	<0.00001
B Cell vs. Memory B Cell (CIBERSORT)	0.54	<0.00001
Macrophages vs. M0 Macrophages (CIBERSORT)	0.23	0.0003
Neutrophils vs. Neutrophils (CIBERSORT)	0.41	<0.00001

**Supplemental Figure 11. Correlations between Immune Deconvolution (this Analysis) and CIBERSORT in HNSCC.** Correlations demonstrated between immune subpopulation single sample gene set enrichment analysis (ssGSEA) used in this study (vertical axis) and an additional validated immune deconvolution algorithm, CIBERSORT, which uses an independent leukocyte gene signature matrix (LM22) (horizontal axis), using the shared available gene expression data between the two data sets. Pearson r-coefficient values are depicted in the figure and table with corresponding p values.  $n=242$ .